# Rapid Diffusion Spectrum Imaging with Partial q-Space Encoding

**A. T. Van[1], R. O'Halloran[1], S. Holdsworth[1], and R. Bammer[1]**
[1]Radiology, Stanford University, Stanford, CA, United States

**INTRODUCTION** – Diffusion spectrum imaging (DSI) [1] is a variant of **q**-space imaging which allows one to measure and interpret the complex diffusion process in microstructures without the necessity of limiting signal models. Despite its great potential, applications of DSI to in *in vivo* studies have been hindered by DSI's long total acquisition time to sample **q**-space. Many studies have tried to speed up DSI, either by using compressed sensing [2], by multiplexing slices in acquisitions [3, 4], or by using signal models and/or signal decomposition [5-7] at the cost of a loss of generality and sometimes a loss of information. The current approach proposes to reduce the total acquisition time of DSI by employing a partial q-space encoding scheme, similar to the partial Fourier encoding in traditional *k*-space imaging. The method does not require any signal modeling and is compatible with previously proposed acquisition-based speed-up techniques [2-4].

**METHODS** – Assuming short pulses [8] or using finite pulses with proper modification of the meaning of the diffusion propagator [9], the **q**-space signal, $S_\Delta(\mathbf{q})$, and the diffusion propagator, $P_\Delta(\mathbf{r})$, are related through the Fourier relationship [8]. Since $P_\Delta(\mathbf{r})$ is a probability density function, it is real. Therefore, from the property of the Fourier transform, we have

$$S_\Delta(-\mathbf{q}) = S_\Delta^*(\mathbf{q}) , \qquad (1)$$

where * is the complex conjugate operation. Here, Equation (1) implies that only half of the **q**-space data needs to be acquired, and the other half can be filled in by the complex conjugate of the acquired half – yielding a 50% speed-up at a cost of a $\sqrt{2}$ loss in SNR. However, to account for the possible **q**-space trajectory errors and shifts caused by background gradients and cross terms, slightly more than half of the **q**-space should be acquired.

• *Data Acquisition:* Both phantom and *in vivo* data were acquired on a GE 1.5 T system with the maximum gradient amplitude of 40mT/m and a slew rate of 150mT/m/ms using an eight-channel head array coil. The pulse sequence was a single-shot echo-planar imaging sequence with spin echo diffusion preparation. The **q**-space encoding parameters were: 9 x 9 x 9 matrix, $g_{max}$ = 37.5 mT/m, $\delta$ = 56 ms, and $\Delta$ = 68 ms corresponding to propagator space resolution of 11 $\mu$m and a field-of-view of 44 $\mu$m. For partial **q**-space sampling one extra **q**-space plane is acquired beyond the q-space center, yielding 44.4% speed-up.

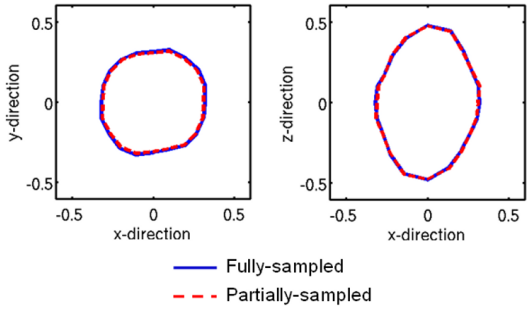


***Fig. 1*** *— Contours of the ODFs generated by fully-sampled (solid lines) and partially-sampled phantom data (dash lines) at (a) z=0 and (b) y=0.*

The phantom was made up of fresh celeries arranged parallel to each other and emerged in pure water. The spatial resolution for the phantom was 2 x 2 x 10 mm$^3$. TE/TR = 144/3000 ms. Without loss of generality, the slice orientation was chosen so that the preferred diffusion direction was through-plane (z-direction).

In the *in vivo* scan a single slice at the level of corpus callosum was acquired with a resolution of 3.75 x 3.75 x 4 mm$^3$. TE/TR = 140/3000 ms. The experiments were approved by our IRB and scanning commenced after written informed consent was obtained from the subjects.

• *Q-Space Data Processing:* Before estimating the propagator, the acquired **q**-space data were low-pass-filtered with a Hanning window to minimize the effect of **q**-space truncation artifacts (i.e. ringing filtered). For partial **q**-space encoding, the missing part of the **q**-space was filled in following Equation (1) before filtering. The propagator was then estimated by taking the 3D Fourier transform of the filtered **q**-space data. To show the accuracy of the partial q-space encoding, besides comparing the propagators of partially and fully q-space sampled data, the commonly used orientation distribution function (ODF) was also employed. The ODFs were computed from the 3D propagator using

$$\mathrm{ODF}(\theta,\varphi) = \int_0^{+\infty} P_\Delta(\rho,\theta,\varphi)\rho^2 \mathrm{d}\rho , \qquad (2)$$

where $P_\Delta(\rho, \theta, \varphi)$ is the value of the estimated propagator in spherical coordinates obtained by 3D cubic interpolation from $P_\Delta(\mathbf{r})$.

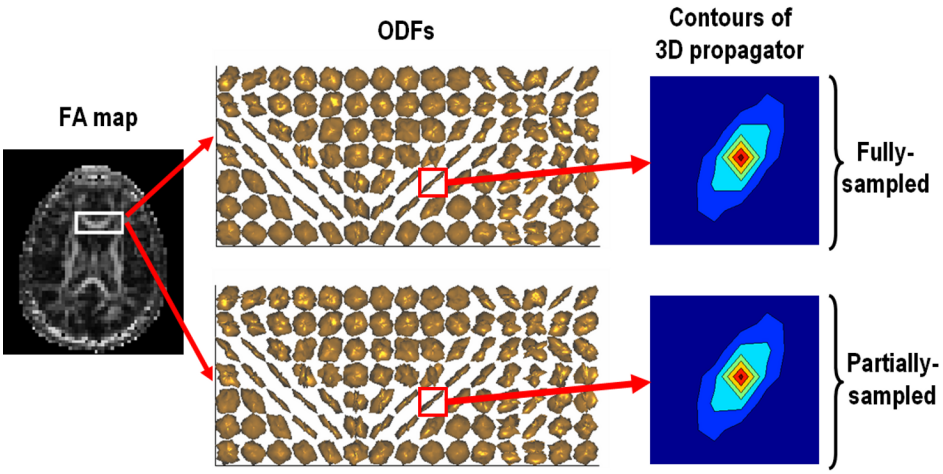


***Fig. 2*** *– In vivo: ODFs (middle panels), and 2D contours of the 3D propagators (right panels) obtained at a region of interest within the corpus callosum using fully-sampled, and partially-sampled **q**-space data.*

**RESULTS** – • *Phantom:* Due to the relatively low anisotropy of the celery phantom (maximum FA of 0.2), the ODFs are predominantly elliptical. Partial **q**-space sampling gave the same ODF as the one generated by full **q**-space sampling. To further illustrate the similarity between the ODFs, the contours of both ODFs are overlaid in Fig.1. • *In vivo*: The middle panels of Fig. 2 show the obtained ODFs in the region of interest pointed out by the white square box on the FA map. No difference was observed between the ODFs generated by partially-sampled **q**-space data and the ODFs generated by fully-sampled **q**-space data. The right panels of Fig. 2 compares the 3D propagators reconstructed from fully-sampled and partially-sampled **q**-space data. The structure of the propagator is well-preserved in the partially-sampled case. Unlike the ODFs, the propagators contain not only the orientation but also the size and shape of the underlying neuronal architectures. By using partial **q**-space encoding, the total acquisition time was reduced by 44.4%. Although complex conjugation was used to fill in the missing **q**-space points in the current work, POCS or homodyne reconstruction can be used together with more than half **q**-space acquisition to ensure accurate reconstruction of the propagator even when any imperfection drives the propagator from being real.

**CONCLUSION** – We have shown that partial **q**-space encoding is an efficient acquisition method for diffusion spectrum imaging. The method is proposed based on the intrinsic property of the diffusion propagator and does not require any signal modeling. Forthcoming work will focus on the combination of partial q-space imaging with the approaches referenced below.

**REFERENCES** – [1] Wedeen et al., MRM. 54, p. 1377-1386, 2005; [2] Menzel et al., ISMRM, p. 1698, 2010; [3] Reese et al., JMRI. 29, p. 517-522, 2009; [4] Setsompop et al., ISMRM, p. 187, 2010; [5] Tuch, MRM. 52, p. 1358-1372, 2004; [6] Assaf et al., NeuroImage. 27, p. 48-58, 2005; [7] Wu et al., NeuroImage. 36, p. 617-629; [8] Callaghan, Clarendon Press, Oxford, 1991; [9] Mitra et al., JMRA. 113, p. 94-101, 1995.

**ACKNOWLEDGEMENTS** – NIH (5R01EB002711, 5R01EB008706, 3R01EB008706S1, 5R01EB006526, 5R21EB006860, 2P41RR009784), Lucas Foundation, and Oak Foundation.